Effect of Friction Stir Welding Parameters on Fatigue Resistance, Weld Quality and Mechanical Properties of Al 6061-T651

Mohamed Ackiel Mohamed
University Kuala Lumpur Malaysia France Institute, Bandar Baru Bangi, Selangor, Malaysia.

Yupiter HP Manurung,
Faculty of Mechanical Engineering, Universiti Teknologi MARA (UiTM), 40450, Shah Alam, Selangor, Malaysia

ABSTRACT

The present work examined the fatigue life cycle, tensile behavior, nugget zone hardness and weld quality of friction stir welded Al 6061-T651 with varying welding parameters. The joining process was conducted with varied process parameters namely the rotational speed and traverse speed on butt joints with plate thickness of 6mm. The experimental method was based on a full factorial design with varied parameters between 350-1400 rpm and 0.2-4.6 mm/s for rotational speed and traverse speed respectively utilizing four levels for each parameter. The fatigue life cycle for each variation was determined. The zone formation and internal weld defects were analyzed using digital x-ray and macroscopically with a designated weld class for each parameter variation. Furthermore, the causes of internal weld defects and the effect of zone formation on tensile strength properties and hardness profile were discussed and concluded. The best mechanical properties are obtained at higher traverse speeds with moderate rotational speed probably owing to the incidence of homogeneous grains and higher heat input. Two parameter variations displayed a combination of good weld class quality and mechanical properties namely rotation speed 950rpm with 4.6 mm/s traverse speed as well as 650 rpm rotation speed with 2.4 mm/s traverse speed. An increase in the nugget hardness shows an increment in the fatigue life.

Keywords: *Friction Stir Welding, AA6061, Full Factorial Design, Weld Quality, Mechanical Properties, Fatigue Life.*

ISSN 1823-5514, eISSN 2550-164X
Received for review: 2016-11-07
Accepted for publication: 2017-02-16
Published: 2017-05-15

Introduction

Leave Friction stir welding (FSW) has proven to be an effective and ecologic solid state joining process eliminating material waste and detrimental gas emissions as well as evading radiation normally associated with the commonly used fusion welding process. Since the innovative inception of FSW by The Welding Institute (TWI) Ltd, Cambridge UK in 1991, the primary research and industrial interest for this process has been for butt and lap joining of aluminum alloys, especially the 2XXX, 6XXX and 7XXX series of heat treatable aluminum alloys, usually considered to be ‘‘unweldable” with the 6XXX series being the more favorable choice due to its reasonable strength and possession of excellent welding characteristics [1-2].

FSW has made the joining of similar and dissimilar aluminum alloy from the 6XXX series easier and more reliable due to the diminishing of continuous problems caused by heat generated during the conventional joining process such as severe softening in the heat affected zone (HAZ) because of reversion (dissolution) of Mg2Si precipitates during weld thermal cycle [5]. Furthermore, the many advantages offered by FSW compared to fusion welding techniques due to its nature of not reaching the melting temperature such as finer microstructure in the stir zone, very minimal distortion and shrinkage from solidification, minimal stress concentrations and weld defects instigated extensive usage of aluminum alloy in a wide range of industrial applications such as in the aerospace, marine, automotive and the most recent, being the off shore industries [9].

The rapid development of FSW technology due to the extensive application in various industries has made the determination of the ideal parameters to be utilized in accordance to specific needs such as the fatigue life, tensile strength, hardness combined with weld quality when joining material of various thicknesses and tempering conditions on area deserving wide focus.

Although numerous investigations have been conducted involving Al6061 [6-10], there has been no attempt yet to relate the effect of varying the FSW governing parameters to a multi objective outcome of several desired conditions in Al6061-T651 butt joint plates by designating a weld quality class with each varied parameter as well determining the effect of increasing hardness on fatigue life. Conversely, numerous optimization and modeling investigations focusing on the FSW process parameter effects and influence by forerunners have mainly been concentrating on single quality characteristics which may deteriorate other characteristics. Although some researchers have attempted multi objective optimization, mechanical properties with fatigue and weld quality as combined outcomes is yet to be determined.

Most of the published papers are focused on the effect of FSW parameters and tool profiles on tensile properties and microstructure formation or the hardness profile. However, the range of industrial applications involving FSW aluminum alloy requires the overall quality for any specific joint or product; hence, making multi objective quality outcome due to the influence of FSW governing parameters a necessity. The present research attempts to determine the influence of the governing FSW parameters namely the rotational and welding speed for Al6061-T651 6mm thick butt joint under simultaneous consideration of multiple considerations such as the fatigue life, tensile strength, hardness value and weld quality class in accordance to the acceptance limit outlined in the industrial standards for friction stir welding, AWS D17.3 [14] as these properties are important in applying post welded fatigue enhancement methods such as High Frequency Mechanical Impact (HFMI) treatments.

Experimental Procedure

In the present study, Al6061-T651 plates were used. The chemical composition of the plate is given in Table 1. Two aluminum plates of 250×100×6 mm (length, width, and thickness) were placed on a flat copper plate in a butt joint arrangement with straight edge preparation. Before placing the plates, the edges of the plates were properly cleaned by using acetone. The FSW was accomplished on the vertical head milling machine with the position of the tool fixed relative to the surface of the plate. The workpiece was firmly clamped to the bed and a cylindrical tool was plunged into the selected area of the material for sufficient time in order to plasticize around the pin.

Table 1: Chemical composition of workpiece

Percent Composition (%)	**Si**	**Fe**	**Cu**	**Mn**	**Mg**	**Cr**	**Ni**	**Zn**	**Ti**	**Ga**	**V**
	0.74	0.44	0.22	0.034	1.03	0.054	0.007	0.029	0.011	0.014	0.021

The welding was executed using constant axial loading, 8KN with variable rotational and traverse speeds. Based on the thickness of the plate, the length of the pin was appropriately selected. The ratio of diameters of the shoulder and pin was maintained constant in order to make the required pressure not only for reconsolidation of material but also to avoid the escape of material during welding. The friction welding process and tool profile used are depicted in Figure 1 (a) and (b).

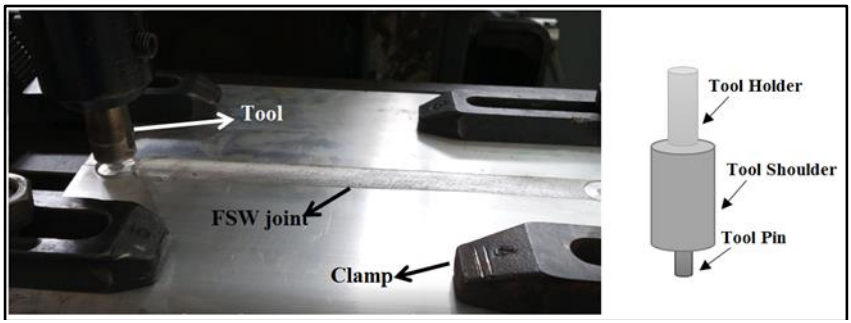

(a) (b)

Figure 1: Friction stir welding process and Tool profile (a) Friction stir welding process, (b) Tool profile

The tool used had dimensions of 18mm shoulder diameter and a shoulder length of 24mm with a cylindrical pin size of 6mm diameter and 5.5mm pin length. The holder was 20mm in length and measured 10mm in the diameter. The tool was fabricated using H-13, an air hardening 5% chromium tool steel which is an excellent choice for a wide range of hot work and cold work applications.

The effect of welding parameters on the joint quality was observed through defect analysis on FSW specimens using a nano-focus digital x-ray with an aim of fabricating defect-free joints. The internal defects in FSW joints were further observed through macrostructures at different parameter combinations. The weld quality of the joints were then classified into three classes namely A1, A2 and A3 as per quality characteristic classification in AWS D17.3 [13] class A weld quality based on the geometrical conditions of the defects found on each run. The weld joints from each run were classified according to the designated weld class. The internal defects, weld class and designated scores used are presented in Table 2.

Table 2: Acceptance level for weld quality classes in accordance to AWS D17.3 [3] and the designated ratings

Type of Defects	**AWS D17.3 Class A**	**Proposed Classification accordingly to AWSD17.3 Class A**		
		Class A1 (Rating =3)	Class A2 (Rating =2)	Class A3 (Rating=1)
Incomplete joint penetration	None	None	None	None
Inclusion (individual size)	1.5mm	0-0.5mm	0.51-1.0mm	1.1-1.5mm

Internal Cavity or cavity open to the surface	None	None	None	None
Angular distortion	3 Degrees	1 Degrees	2 Degrees	3 Degrees
Individual defect (maximum depth)	0.76mm	0-0.25mm	0.26-0.5mm	0.5-0.76mm
Accumulated length of underfill defect of any 3	5.1mm	0-2.5mm	2.6-4.0mm	4.1-5.1mm
Weld flash	Shall be removed	Shall be removed	Shall be removed	Shall be removed
Overlap	Shall be removed	Shall be removed	Shall be removed	Shall be removed

Specimens were taken from each welded plate for fatigue test, tensile, hardness tests and macro profile. Before hardness tests were performed, samples were prepared by the usual metallurgical polishing methods and etched with Keller's reagent while weld zone was captured using a metallurgical microscope interfaced with an image analysis system. Three tensile specimens were taken from the same welded plate for each variation. Tensile tests were performed under a cross head speed of 5 mm/min according to the EN-895-2002 standard. The room temperature tensile strength of the base and the friction stir processed sheet was evaluated by conducting tensile test on a 250KN Instron universal testing machine. A high resolution extensometer was used during uniaxial tensile tests.

The hardness field was established in the midthickness (middle level) of the cross section of the weld seam according to the ISO 6507-2 standard with 3 measured points in the nugget zone using a Struers Duramin Micro-Vickers Hardness test machine with a 1kgf load. Fatigue tests were conducted using a universal Instron testing machine with a load ratio of R=0.1 and 20 Hz frequency. Three fatigue test specimens for each variation were prepared using a milling machine in accordance to the size described in ISO/TR 14345:2012(E) for axial loading. A maximum load of 80 percent from the ultimate tensile strength for each variation was used in the tests.

Result and Discussion

Macrostructure and weld quality

The variations in traverse and rotation speeds used in this study is compiled below in a process map for Al 6061-T651 and presented in Figure 2. This figure indicates that a considerably large range of processing parameters is available for FSW of Al 6061-T651. Nano-focus digital x-ray was used to examine the defects present in each parameter variation before conducting

destructive testing of macrographically to examine the variations which indicated the presence of internal defects. Figure 3 (a-c) depicts the digital x-ray images obtained for specimens that were beyond acceptance criteria, specimen with defects but within acceptance dimensions and defect free FSW joins.

The rotation speed of 950 rpm produced the best set of quality weld joints throughout a variation of traverse speeds and produced a joint with excellent quality with superior mechanical properties at a traverse speed of 4.6mm/s. The worst performing rotation speed was 1400 rpm with 2 weld joints being rejected due to displaying weld defects beyond the acceptance limit. Conversely in general, higher traverse speeds between the ranges of 2.4-4.6 mm/s displayed better overall joint quality with lesser weld defects compared to the lower traverse speed of below 2.4mm/s. However, higher traverse speeds with 1400rpm produced weld joints with numerous defects.

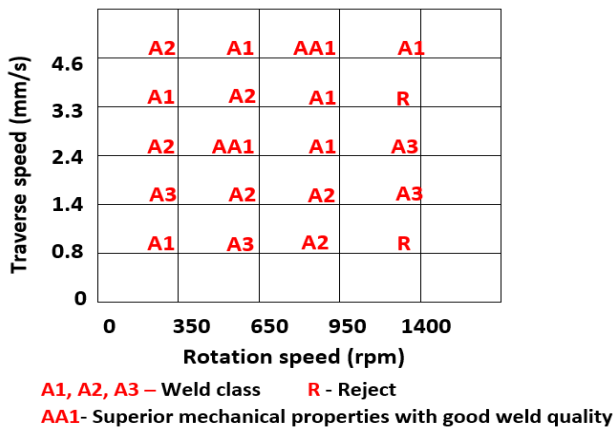

Figure 2: Process map weld quality class classification in accordance to weld quality class A as defined in AWS D17.3 of present study.

Defects such as kissing bond, pin hole, flash and zigzag were detected in the macrostructures. The defects areas are depicted in Figure 4 (a-c). The defects were formed as a result of insufficient heat input caused by higher traverse speed as well as low rotation speeds or an unsuitable combination of both. Lower traverse speeds and higher rotation speeds also influenced several weld defects such as excessive flash.

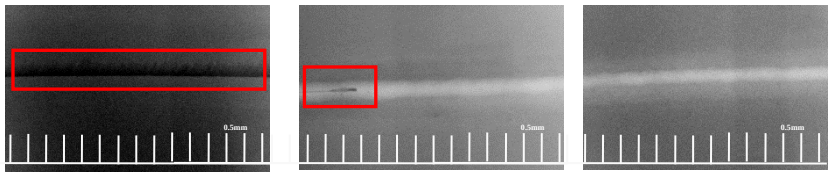

(a) (b) (c)

Figure 3: Digital x-ray quality inspection showing (a) Specimen with tunnel beyond acceptance criteria, (b) Specimen with wormhole within accepted dimensions, (c) Defect free specimen

The weld joints were visually inspected for weld defects and the macrostructure was further investigated for internal flaws. The joints according to the parameter variations were classified into three different weld classes as described in Table 2. Three specimens were completely rejected due to the weld defects being larger than the acceptance level. Joints with higher rotation speeds namely 1400 rpm had seemingly the most number of defects beyond the acceptance criteria.

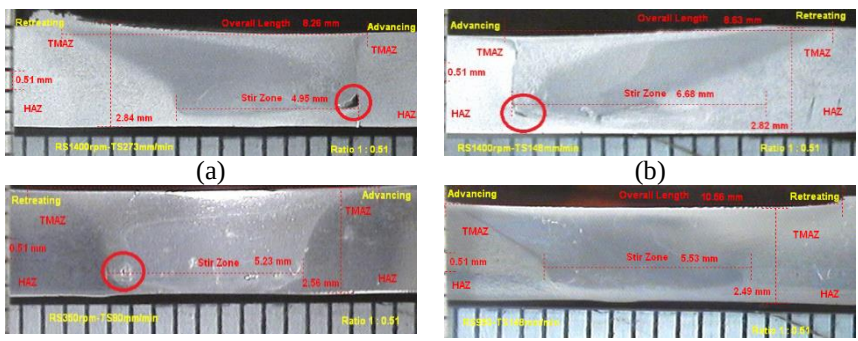

(a) (b)

(c) (d)

Figure 4: Internal weld defects found in different specimens of parameter combinations: (a) Piping defect, (b) Tunnel defect, (c) Pin hole, (d) Defect free weld

Tensile properties

The tensile properties of friction stir welded Al 6061-T651 with variable rotation and traverse speed is depicted in Figure 5(a) and (b). The data shown in Figure 5 represents the value from three tensile tests conducted with the average value calculated for each run and all the data were obtained in the defect-free area.

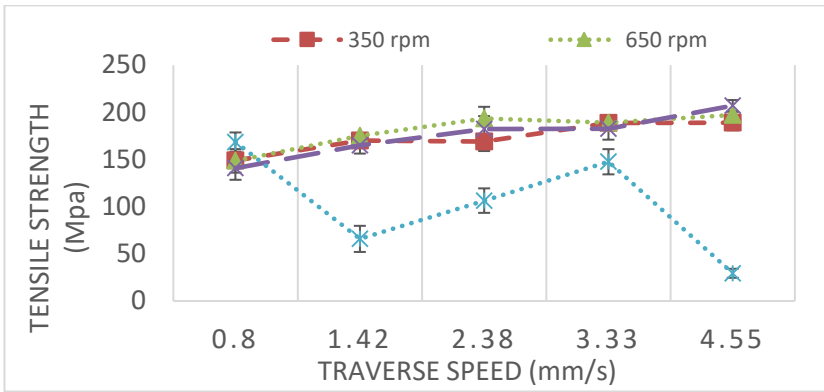

(a)

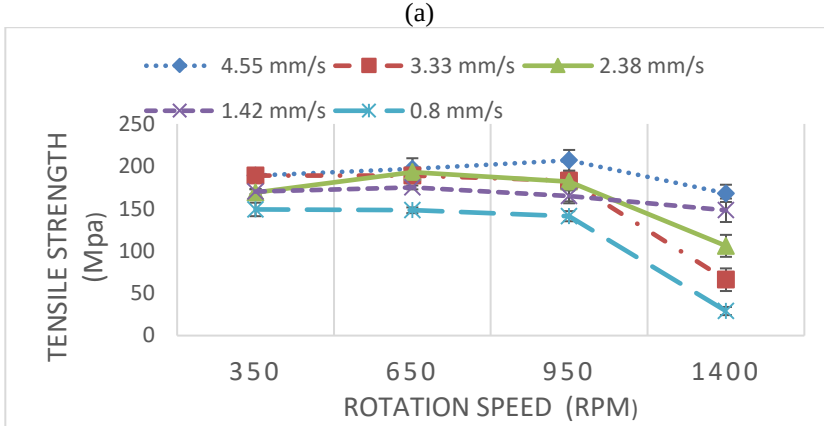

(b)

Figure 5: Tensile strength of varied FSW parameters: (a) Constant rotation speed and increased traverse speed with Error bars indicating a 95% confidence limit, (b) Constant traverse speed and increased rotation speed with Error bars indicating a 95% confidence limit

Considering the best tensile property of friction-stir-welded Al 6061-T651 plate, the yield and ultimate tensile strengths were reduced for 40 and 23 percent, respectively with respect to the parent material. At constant rotating speed with increased traverse speed, the tensile strength tended to increase in a similar pattern for all rotation speeds utilized except for rpm 1400 which showed significant changes with a sharp increment in the beginning then slightly descending before a further final increase in varied values of tensile strengths. Slower traverse speeds with various combinations of rotation speeds tended to provide a satisfactory joint strength of 50 to 60 percent of the base material tensile strength.

Table 3: Tensile test failure location of specimens with different parameter variations.

Traverse speed (mm/min)	Rotation speed (rpm)	Specimen 1	Specimen 2	Specimen 3
		Location of crack		
49	350	TMAZ	TMAZ	TMAZ
	650	TMAZ	WELD NUGGET	TMAZ
	950	HAZ	HAZ	HAZ
	1400	HAZ	HAZ	HAZ
90	350	TMAZ	TMAZ	TMAZ
	650	TMAZ	TMAZ	TMAZ
	950	WELD NUGGET	WELD NUGGET	WELD NUGGET
	1400	HAZ	TMAZ	TMAZ
148	350	TMAZ	TMAZ	TMAZ
	650	HAZ	HAZ	HAZ
	950	HAZ	HAZ	HAZ
	1400	TMAZ	TMAZ	TMAZ
203	350	TMAZ	TMAZ	TMAZ
	650	HAZ	HAZ	HAZ
	950	WELD NUGGET	WELD NUGGET	WELD NUGGET
	1400	TMAZ	TMAZ	TMAZ
273	350	HAZ	HAZ	HAZ
	650	TMAZ	TMAZ	TMAZ
	950	HAZ	HAZ	HAZ
	1400	TMAZ	TMAZ	TMAZ

Increasing the rotation speed while maintaining the traverse speed showed a gradual increase in the tensile strength for all traverse speeds with the traverse speed of 0.8 mm/s having the lowest tensile strength distribution. However, upon reaching the highest tensile strength value at 950 rpm, the magnitude of the tensile strength plunges down sharply when the rotation speed was further increased to 1400 rpm for all traverse speeds. A combination of the lowest traverse speed and highest rotation speed seemingly gave the lowest value of tensile strength. A moderate rotation speed of 950 rpm with the highest value of traverse speed at 4.55 mm/s resulted in obtaining the highest magnitude for the joint tensile strength. These trends are summarized in Figures 5(a) and (b).

It is important to note that the ultimate tensile strength increases with escalating traverse speeds due to the generation of sufficient heat input to swirl and mix the material plastically. The ductility is also marginally

increasing when the traverse speed is increased. The main reason for this behavior is the restoration of the ductility by recrystallization mechanism in addition to the increment of the grain size due to the higher amount of heat generation occurring during higher traverse speeds. The results also affirm that at a higher traverse speed with moderate rotations speeds, both the tensile strength and ductility are marginally higher as shown in Figure 5a. This is an analog of the earlier observation made by [11-12].

Table 3 shows the tensile test specimens failure locations obtained from the friction stir welded joints with different parameters variations. The percentage of tensile failure at the region of TMAZ is 56.67% while the percentage of the tensile failure in the region HAZ is 36.67%. The lowest location of failure occurred at the region weld nugget contributing a total percentage of 6.7%. The higher percentage of fracture in the TMAZ region is attributed to the temperature and deformation experienced by this region without recrystallization occurring due to insufficient deformation strain [15]. The HAZ region experiences less fracture during the tensile tests as a result of undergoing a thermal cycle without experiencing any plastic deformation. The generation of a recrystallized fine-grained microstructure within stirred zone makes this region less vulnerable to fracture unless fabricated with unsuitable rotational and traverse speeds which cause turbulence, destroying the regular flow behavior [15-16].

Hardness profile

The hardness measurements were performed throughout the cross sectional area of the FSW Al6061-T561 butt joint spanning for all the weld zones namely the nugget zone, thermo-mechanical affected zone, heat affected zone and the parent material.

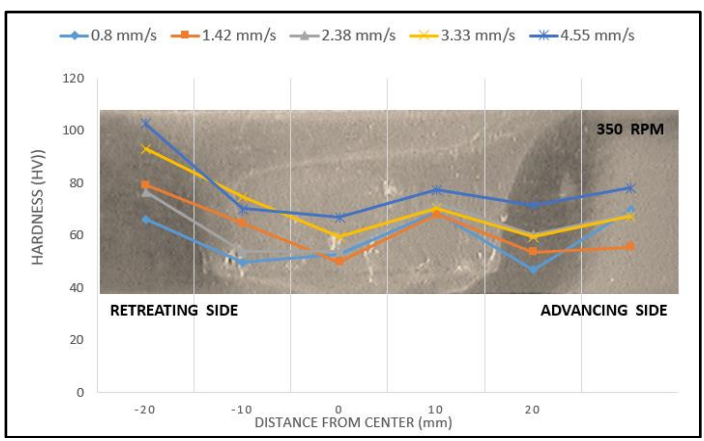

(a)

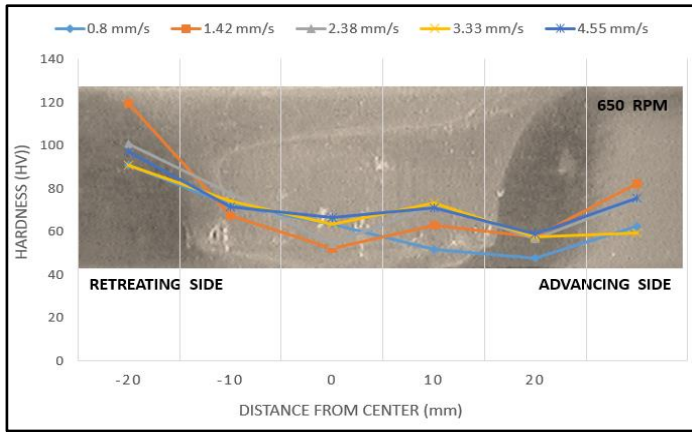
0.8 mm/s
1.42 mm/s
2.38 mm/s
3.33 mm/s
4.55 mm/s
650 RPM
HARDNESS (HV))
RETREATING SIDE
ADVANCING SIDE
DISTANCE FROM CENTER (mm)

(b)

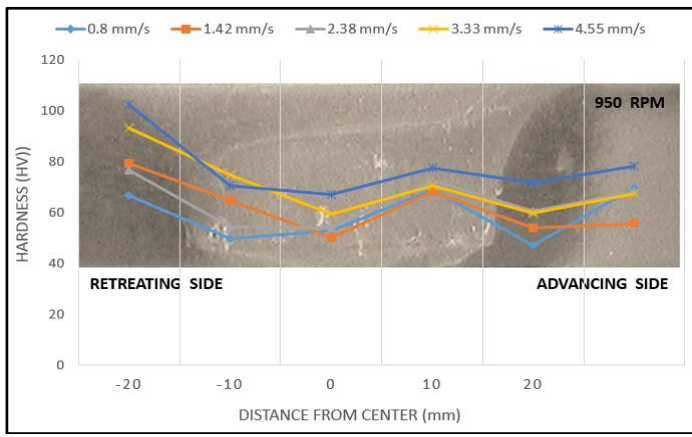
0.8 mm/s
1.42 mm/s
2.38 mm/s
3.33 mm/s
4.55 mm/s
950 RPM
HARDNESS (HV))
RETREATING SIDE
ADVANCING SIDE
DISTANCE FROM CENTER (mm)

(c)

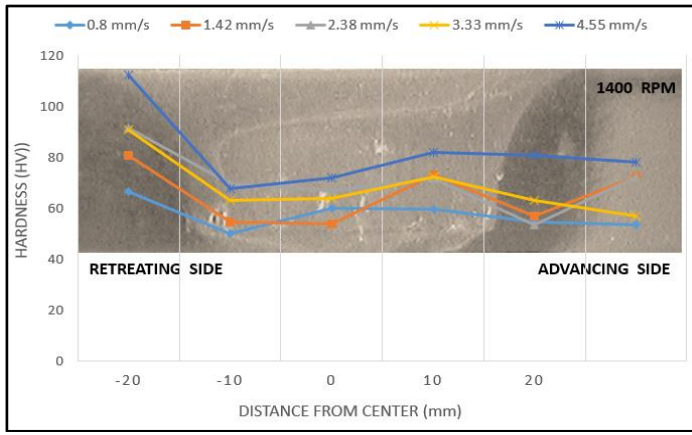

(d)

Figure 6: Vickers hardness profiles in the weld zone and parent material for different variations of rotations speed (a) 350 rpm (b) 650 rpm (c) 950 rpm and (d) 1400 rpm

The hardness for these zones was measured both in the retreating and advancing sides. Horizontal profiles of Vickers hardness in the weld and parent metal with varied traverse speed with constant rotation speeds are shown in Figure 6 (a-d). It is found that the hardness of base material varies between 105 and 110 HV. Compared to the parent material, dynamic recrystallization in FSW joints plays a major role in the elimination of strain hardening which significantly softens the weld zone. This in turn causes a decrement of the hardness values in the thermomechanically affected zone as well in the vicinity of the weld nugget. Hardness values ranging from 50-80 HV was observed due to severe softening behavior in the vicinity of the NZ borders of both AS and RS [16].

However, the width of the severe softening region on AS is evidently wider than that on RS. It is known that AA6061 contains various strengthening precipitates such as β-Mg_2Si. During the welding process, both dissolution and growth of the precipitates which are mentioned above occur due to the heat cycle. The high density of fine needle shaped β" precipitate is the main strengthening source for AA6061-T6, but it is a metastable transient phase and may be dissolved and evolved to β" and β-Mg_2Si phase during the welding [21]. It is likely that the β" and β-Mg_2Si precipitates in the middle part of NZ are dissolved by the heat generated in the welding process. Consequently, GP zones precipitate in the following cooling of the weld. Thus, the softening of NZ occurred.

At a constant rotational speed, an increment in the traverse speed caused an increment in the hardness values in NZ as well as the TMAZ in the

advancing side. Significant increments in these zones were observed in the rotation speed with higher values namely 1400 rpm and 950 rpm. Increasing rotations speeds with constant traverse speed showed an increment in the NZ as well as the TMAZ, with the rotation speed of 1400 rpm recording the highest value of Vickers hardness profile speed.

The rotation speeds of 650 rpm depicted a 'bowl' shape and 950 rpm formed a typical 'W' shaped hardness profile while the speed of 1400 rpm formed a mixture of 'W' and 'bowl' shaped hardness profiles. Compared to the base material, the hardness value drops significantly in thermomechanically affected zone and increases slightly in the nugget zone. This pattern is similar in both retreating and advancing sides. However, the advancing side shows a slightly higher magnitude in hardness compared to the retreating side. This is closely attributed to the appearance of fine-grain size in the nugget zone at higher traverse.

All four rotation speeds utilized depict a typical 'W' shaped hardness profile except the lowest rotation speed, namely 350 rpm which forms a 'V' shaped hardness profile. Compared to the base material, the hardness value drops significantly in thermomechanically affected zone and increases slightly in the nugget zone. This pattern is similar in both retreating and advancing sides. However, the advancing side shows a slightly higher magnitude in hardness compared to the retreating side. The hardness values increase considerably by increasing rotation speed, with the rotation speed of 1400 rpm recording the highest value of Vickers hardness profile. The hardness also tends to increase with increasing traverse speed regardless of the rotation speeds used.

This is closely attributed to the appearance of fine-grain size in the nugget zone at higher traverse speed [17-18]. However, Figure 5 and Figure 6 demonstrate that the tensile property and hardness profile of friction-stir-welded Al 6061-T651 alloy, as well as the soundness of welding, may vary greatly with different welding parameters. Two parameter combinations namely rotation speed 950rpm with 4.6 mm/s traverse speed as well as 650 rpm rotation speed with 2.4 mm/s traverse speed showed excellent tensile properties combined with reasonable hardness values without any visual weld defects.

Fatigue life cycle

Fatigue tests were conducted to obtain the life cycle to failure for each variation. Samples chosen were ensured defect free prior to testing. As the fatigue test results showed huge scatter, linear regression with a 50 percent confidence level was used to describe the distribution pattern as depicted in Figure 7.

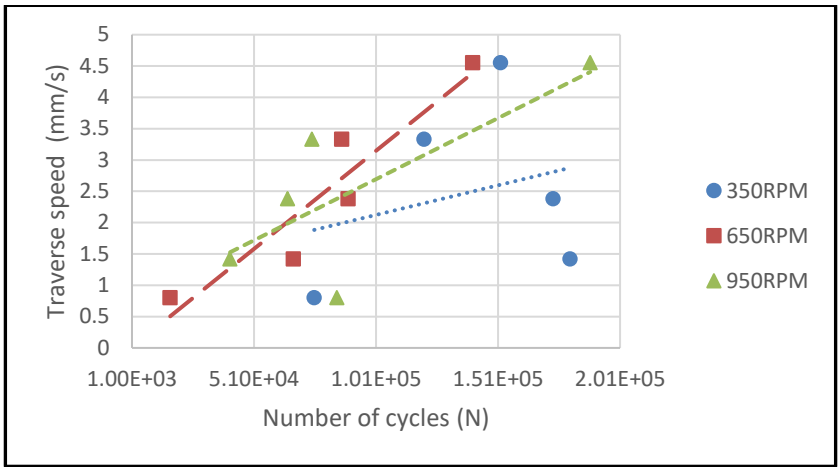

Figure 7: Fatigue life cycle to failure of varied FSW parameters for constant rotation speed and increased traverse speed.

Increasing the traverse speed while maintaining the rotation speed showed a slight increase in the fatigue life cycle with a lower rotation speed of 350 rpm while the rotation speeds of 650 rpm and 950 rpm showed a significant increase. The lower rotation speed of 350rpm with a speed exceeding 1 mm/s resulted in an averagely higher fatigue life compared to the other variations. The highest traverse speed of 4.55 mm/s resulted in a relatively higher fatigue life for all the rotation speeds, namely 350 rpm, 650 rpm and 950 rpm. The highest life cycle to failure of 188768 cycles was recorded at combination of rotations speed of 950 rpm and a traverse speed of 4.55 mm/s.

Most of the cracks occurred initiated in the HAZ and the TMAZ regardless of the number of cycles to failure. This is attributed to the minima hardness values being recorded in this region. This result affirms the revelation by [19-20]. The correlation between fatigue life and hardness values obtained in the nugget zone is displayed in figure 8. It is also noteworthy that the fatigue life cycle is marginally proportional to the hardness values obtained where an increase in hardness shows a slight increment in the life cycles. Lower hardness values obtained from the parameter variation contributed to lower fatigue life cycles although some variations with temperate hardness values resulted in higher fatigue life cycles. The reason for this is not clear, as fatigue life cycles in welded structures habitually ascribes scatter.

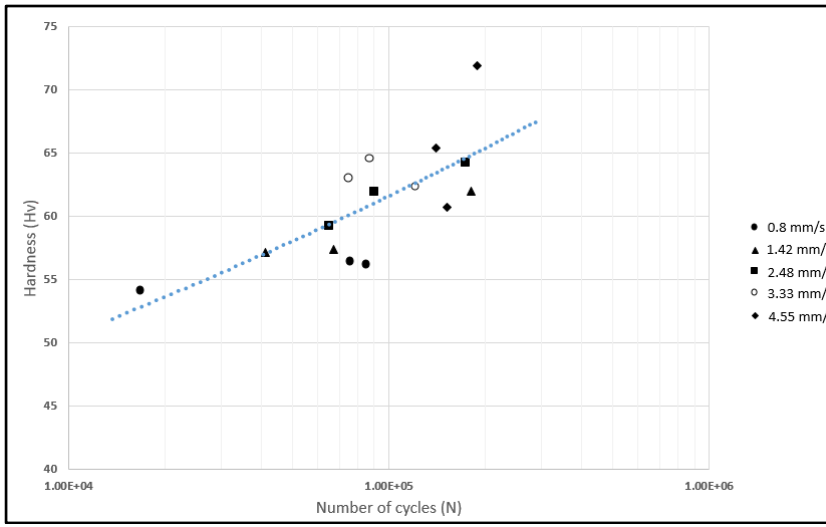

Figure 8: Fatigue life cycle to failure correlation to nugget zone hardness of varied FSW parameters

Conclusion

The following conclusions were drawn from the present investigation:

1. Increased traverse speeds tends to increase the ultimate tensile strength and fatigue life cycle.
2. Increasing traverse speed as well as the rotation speed significantly increases the hardness value.
3. The best mechanical properties are obtained at higher traverse speeds with moderate rotational speed owing to the incidence of homogeneous grains and higher heat input. Inadequate heat inputs causes weld defects to form in the weld zone.
4. An increment in hardness values consequences a moderate increment in fatigue life cycle.
5. Two parameter variations display a combination of good weld quality and mechanical properties namely rotation speed 950rpm with 4.6 mm/s traverse speed as well as 650 rpm rotation speed with 2.4 mm/s traverse speed.

References

[1] Properties of Wrought Aluminum and Aluminum Alloys: 6061 Alclad 6061", *Properties and Selection: Nonferrous Alloys and Special-*

Purpose Materials, Vol 2, ASM Handbook, ASM International, 1990, p. 102-103

[2] Z. S. Mishra and Z. Y. Ma, "Friction stir welding and processing," *Materials Science and Engineering: R: Reports*, vol. 50, no. 1–2, pp. 1–78, Aug. 2005.

[3] S. R. Ren, Z. Y. Ma, and L. Q. Chen, "Effect of welding parameters on tensile properties and fracture behavior of friction stir welded Al–Mg–Si alloy," *Scripta Materialia*, vol. 56, no. 1, pp. 69–72, Jan. 2007.

[4] Jauhari Tahir Khairuddin, Jamaluddin Abdullah, Zuhailawati Hussain and Indra Putra Almanar (2012). Principles and Thermo-Mechanical Model of Friction Stir Welding, Welding Processes, Dr. Radovan Kovacevic (Ed.), ISBN: 978-953-51-0854-2, InTech, DOI: 10.5772/50156.

[5] K. Elangovan, V. Balasubramanian, and S. Babu, "Predicting tensile strength of friction stir welded AA6061 aluminum alloy joints by a mathematical model," *Materials & Design*, vol. 30, no. 1, pp. 188–193, Jan. 2009.

[6] D. M. Rodrigues, a. Loureiro, C. Leitao, R. M. Leal, B. M. Chaparro, and P. Vilaça, "Influence of friction stir welding parameters on the microstructural and mechanical properties of AA 6016-T4 thin welds," *Materials & Design*, vol. 30, no. 6, pp. 1913–1921, Jun. 2009.

[7] A.Heidarzadeh, H. Khodaverdizadeh, a. Mahmoudi, and E. Nazari, "Tensile behavior of friction stir welded AA 6061-T4 aluminum alloy joints," *Materials & Design*, vol. 37, pp. 166–173, May 2012.

[8] S. Lim, S. Kim, C. Lee, and S. Kim, "Tensile Behavior of Friction-Stir-Welded Al 6061-T651," vol. 35, no. September, pp. 2829–2835, 2004.

[9] C. Dawes, W. Thomas, TWI Bulletin 6, November/December 1995, p. 124.

[10] B. London, M. Mahoney, B. Bingel, M. Calabrese, D.Waldron, in: Proceedings of the Third International Symposium on Friction Stir Welding, Kobe, Japan, 27–28 September, 2001.

[11] N. T. Kumbhar and K. Bhanumurthy*, *Asian J. Exp. Sci., Vol. 22, No. 2, 2008; 63-74*

[12] M. Peel, A. Steuwer, M. Preuss, P.J. Withers, Acta Mater. 51 (2003) 4791.

[13] M. Ericsson and R. Sandström, "Fatigue of Friction Stir Welded AlMgSi-Alloy 6082," *Materials Science Forum*, vol. 331–337, pp. 1787–1792, 2000.

[14] AWS D17.3/D17.3M:2010 Specification for Friction Stir Welding of Aluminum Alloys for Aerospace Applications

[15] Lim S, Kim S, Lee C G, Kim S. Tensile behavior of friction-stir-welded Al 6061-T651 [J]. Metall Mater Trans A, 2004, 35: 2829_2835.
[16] Elangovan K, Balasubramanian V. Influences of tool pin profile and tool shoulder diameter on the formation of friction stir processing zone in AA6061 aluminum alloy [J]. Material Design 2008, 293: 362_373.
[17] Barcellona A, Buffa G, Fratini L, Palmeri D. On microstructural phenomena occurring in friction stir welding of aluminum alloys [J]. J Mater Processing Technology, 2006, 177: 340_343.
[18] Sato Y. S., Takauchi H., Park S. H. C., Kokawa H. Characteristics of the kissing-bond in friction stir welded Al alloy 1050 [J]. Mater Sci Eng A, 2005, 405: 333_338.
[19] Montgomery D C. Design and analysis of experiments [J]. 2nd ed. New York: Wiley, 1984.
[20] Rajakumar S, Muralidharan C, Balasubramanian V. Establishing empirical relationships to predict grain size and tensile strength of friction stir welded AA 6061-T6 aluminum alloy joints [J]. Transactions of Nonferrous Metals Society of China, 2010, 20: 1863_1872.
[21] Y. Uematsu a,*, K. Tokaji a, H. Shibata b, Y. Tozaki b, T. Ohmune. Fatigue behaviour of friction stir welds without neither welding flash nor flaw in several aluminum alloys [J] International Journal of Fatigue 31 (2009) 1443–1453